J. N. Am. Benthol. Soc., 1999, 18(2):199–221

A coupled field and modeling approach for the analysis of nitrogen cycling in streams

WILFRED M. WOLLHEIM[1], BRUCE J. PETERSON, LINDA A. DEEGAN, MICHELE BAHR, AND JOHN E. HOBBIE

The Ecosystems Center, Marine Biological Laboratory, Woods Hole, Massachusetts 02543 USA

DAVID JONES

3660 Kent Road, Stow, Ohio 44224 USA

WILLIAM B. BOWDEN[2]

Department of Natural Resources, University of New Hampshire, Durham, New Hampshire 03820, USA

ANNE E. HERSHEY[3]

Department of Biology, University of Minnesota-Duluth, Duluth, Minnesota 55812 USA

GEORGE W. KLING

Department of Biology, University of Michigan, Ann Arbor, Michigan 48109 USA

MICHAEL C. MILLER

Department of Biological Sciences, University of Cincinnati, Cincinnati, Ohio 45221 USA

Abstract. The stable isotope stream tracer model (SISTM) calculates the expected ^{15}N content in various stream ecosystem N compartments over distance and time during and after ^{15}N additions to streams. SISTM is a steady state compartment model that predicts $\delta^{15}N$ values based on N stocks and fluxes and the experimental rate of ^{15}N addition. Predicted $\delta^{15}N$ values are compared with observed $\delta^{15}N$ values from a field tracer addition to evaluate our understanding of the N cycle. We demonstrated the use of this tool with information collected from field measurements and a 6-wk ^{15}N-NH_4^+ addition to the Kuparuk River, Alaska, during the summer of 1991. SISTM was used to run a series of model calibrations that reflected increased information as the experiment progressed. Results of an a priori calibration (using pre-1991 data) yielded a predicted NH_4^+ uptake length (S_w) of 5.2 km compared with the observed S_w of 0.84 km, and underestimated the $\delta^{15}N$ values of biota in all cases. When discharge and NH_4^+ concentrations measured during the 1991 experiment were added (model calibration Update 1), the predicted S_w dropped to 0.44 km, indicating that the modeled fluxes overestimated the rate of NH_4^+ removal by the stream bottom. Adding N stocks and fluxes measured during the tracer addition (Update 2) did not improve predicted S_w, indicating faulty assumptions in our a priori calibration. The observed isotope data were used to estimate the form (NH_4^+ vs NO_3^-) of N taken up by primary producers and to improve our representation of the epilithon compartment (Update 3). Including this information brought the predicted S_w to 0.71 km compared with the observed 0.84 km, and resulted in a reasonable correspondence between predicted and observed $\delta^{15}N$ values over the 6-wk addition. SISTM can be used as a framework to 1) summarize N-cycle information prior to a tracer addition, 2) generate testable predictions for field isotope studies, 3) improve our understanding of the N cycle using the field isotope data as constraints on flux estimates, and 4) explore hypothetical N-cycle characteristics. The combined modeling and field tracer experiment approach efficiently provided a synoptic view of the N cycle in streams and rivers.

Key words: N cycling, compartment model, tracer addition, stable isotope, ^{15}N, uptake length, stream ecosystem.

[1] E-mail address: wollheim@mbl.edu

[2] Present address: Landcare Research, P.O. Box 69, Lincoln 8152 New Zealand

[3] Present address: Department of Biology, University of North Carolina–Greensboro, Greensboro, North Carolina 27402 USA

The N cycle exerts powerful control over the activity of the biosphere because N supply can limit a wide array of ecosystem processes. Human activity has significantly altered the global N cycle with potentially large implications for ecosystem function (Vitousek 1994, Galloway et al. 1995, Vitousek et al. 1997). For example, N flux via rivers to the sea has increased several fold over the past several decades with severe consequences to river and estuarine ecosystems (Meybeck 1982, Howarth et al. 1996). Consequently, understanding the fate of anthropogenic N is a priority for projecting the impacts of global change. Yet relatively little is known about N uptake, storage, and recycling during riverine transport from uplands to lakes and oceans (Jordan and Waller 1996). Stable isotope tracer additions to whole ecosystems have proven useful for understanding N dynamics in a variety of ecosystems, including forests (Knadelhoffer et al. 1995), lakes (Kling 1994), estuaries (Holmes et al., in press), and streams (Peterson et al. 1997, Hall et al. 1998). We present a simple compartment model that can be used in conjunction with tracer additions to evaluate and improve our understanding of N cycling in stream ecosystems.

Nutrient dynamics in streams have been studied using solute injections of nitrate (NO_3^-), ammonium (NH_4^+), and phosphate (PO_4^{3-}) (Triska et al. 1989a,b, Webster et al. 1991, Marti and Sabater 1996, Valett et al. 1996, Marti et al. 1997), short-term radiotracer additions of ^{32}P (Ball and Hooper 1963, Newbold et al. 1983a, Mulholland et al. 1985), and long-term additions (on the order of weeks) of stable isotopes in the form of ^{15}N-NH_4^+ (Peterson et al. 1997, Hall et al. 1998). Solute injections are useful for determining nutrient retention by streams but cannot readily determine processing mechanisms (Stream Solute Workshop 1990). In contrast, isotope tracers can address both retention and its numerous underlying processes (Newbold et al. 1983a). Because these processes interact during transport, models that incorporate all significant interactions are necessary to understand the observed tracer distribution.

Tracer information can be used to develop models of stream nutrient cycling. For example, rates of P flux between compartments were mathematically derived to best fit data from a ^{32}P addition to Walker Branch, Tennessee (Newbold et al. 1983a). Alternatively, tracers can evaluate nutrient cycling models derived from nontracer information. We initially followed this latter approach in conjunction with a ^{15}N-NH_4^+ addition to the Kuparuk River in 1991 (Peterson et al. 1997). We independently determined N stocks and fluxes of dissolved and sestonic N, total chlorophyll, and organic N on rocks, moss biomass, insect biomass, primary production, and insect growth rates. We then used the stable isotope stream tracer model (SISTM) to predict where, based on these stocks and fluxes, the added tracer should be found over time and distance. Where there was a lack of agreement between measured and predicted $\delta^{15}N$ values, the field isotope data were used to improve or at least constrain certain estimates of fluxes between compartments.

Our goal was to use SISTM as a tool to understand the N cycle in streams. SISTM is neither a simulation model of N cycling response to environmental change, nor a general model of N cycling that can be automatically applied to any site, because it requires specific parameterization with stock and flux data from each stream setting. We feel that this modeling approach, combined with the field tracer addition, is a valuable and necessary prerequisite to development of a more general N-cycle simulation model of stream ecosystems.

We illustrate how SISTM helped to develop understanding of the N cycle of a pristine reach of the upper Kuparuk River in Alaska. SISTM has also been applied to a stream in North Carolina (Hall et al. 1998) and to other streams as part of a Lotic Intersite Nitrogen Experiment (LINX Project, funded by NSF). We undertook a sequence of model calibrations using SISTM that met several objectives in conjunction with a tracer addition. Among these objectives were to: 1) synthesize prior information on the N cycle of a given stream, 2) adjust the general understanding of the N cycle by incorporating actual conditions during the addition (e.g., discharge, nutrient concentration, N stocks), 3) assess our understanding by comparing predicted with observed $\delta^{15}N$ values, 4) use the observed $\delta^{15}N$ data to constrain or derive flux estimates that are otherwise difficult to obtain, and 5) formulate testable hypotheses about N uptake, storage, and transformations. Our overall goal was to achieve a synoptic and quantitative assessment of the N cycle in the study reach.

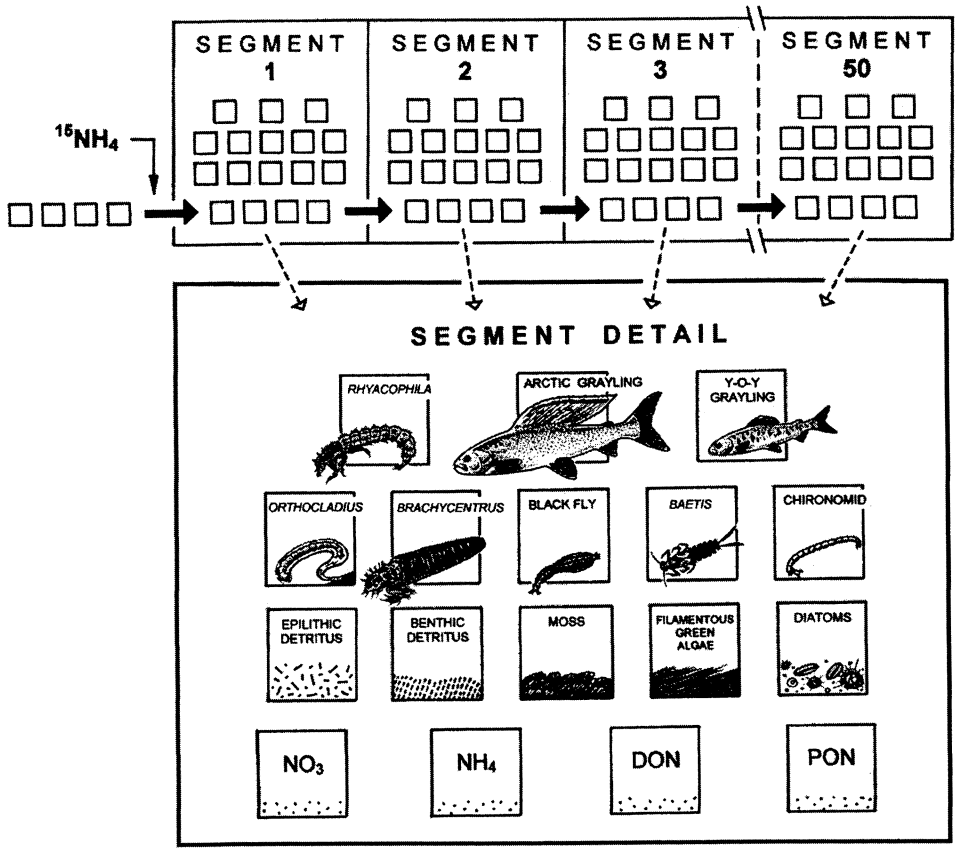

FIG. 1. General design of the stream isotope tracer model (SISTM). The N tracer is added to segment 1 where it is incorporated into the various compartments based on flux of total N. Each segment in the Kuparuk River model consists of 16 compartments (17 in the final version after epilithon was split into diatom and epilithic detritus compartments) including suspended (NH_4^+ = ammonium, NO_3^- = nitrate, DON = dissolved organic nitrogen, PON = particulate organic nitrogen) and benthic stream components. $\delta^{15}N$ values are updated for each compartment per time unit and tracer is transported in the suspended compartments to the next segment where the process is repeated. Y-O-Y = young-of-the-year grayling.

Methods

SISTM model

SISTM computes where a stable isotope tracer (^{15}N-NH_4^+ in our application) added to a stream will reside over time and distance, based on our understanding of the N cycle. ^{15}N-NH_4^+ is added continuously to the 1st of a series of stream segments, each containing an identical set of compartments (N stocks) and N fluxes. For the Kuparuk River, each segment consisted of 16 compartments (17 in the final version after epilithon was split into diatom and epilithic detritus compartments) (Fig. 1). The compartments included dissolved inorganic N (NH_4^+, NO_3^-), dissolved and particulate organic N (DON, PON), the dominant primary producers, invertebrates, fish, and detrital N (Fig. 1).

Fluxes between compartments determine where the added ^{15}N resides in each segment. In each segment and for each time unit, ^{15}N is taken up by the various stream compartments and their $\delta^{15}N$ values are updated according to the following equation:

$$\delta_{t=t+1} = \left(\delta_t \cdot M_A + \sum_{K=1}^{n} (\delta_K \cdot M_{KA})\right) \div \left(M_A + \sum_{K=1}^{n} M_{KA}\right)$$

where $\delta_{t=t+1}$ = the new $\delta^{15}N$ of compartment A at time t = t + 1, M_A = mass of total N in compartment A at time t, δ_t = $\delta^{15}N$ of compartment A at time t, M_{KA} = mass of total N flux from compartment K to compartment A, δ_K = the $\delta^{15}N$ value of compartment K at time t, and n = number of compartments that have fluxes to compartment A, including any advective inputs from upstream. Thus, each compartment contains a new $\delta^{15}N$ value that is a function of its total N and $\delta^{15}N$ content at time t updated by the mass and $\delta^{15}N$ of all N fluxes leading to it between t and t + 1.

After all fluxes within a segment are accounted for, dissolved (NH_4^+, NO_3^-, DON) and suspended (PON) compartments containing updated $\delta^{15}N$ values flow to the next downstream segment. The ^{15}N values of these inputs from the upstream segment are incorporated using the same set of N fluxes as the previous segment. Each segment is identical and represents a typical pool/riffle sequence and contains the same N stocks and fluxes. Fluxes are parameterized in mass per time unit (usually days), with each time unit broken into 20 sub-time units by SISTM to account for increased tracer flux as tracer slowly accumulates within compartments during a time unit. Once $\delta^{15}N$ has been updated for all segments within a sub-time unit, SISTM returns to segment 1 for the next sub-time unit.

Fluxes in SISTM are constant amounts (zero-order), making this a steady state representation of N flow. Stocks can increase or decrease based on the balance between inputs and outputs, but no mechanisms in the model control the rate of change. Imbalances in stream bottom compartments accumulate over time, whereas imbalances in the dissolved or suspended compartments accumulate with distance. Compartments with unequal inputs and outputs must be carefully calibrated as there are no feedbacks in SISTM to alter flux rates as N stocks reach unrealistically high or low levels.

SISTM treats each segment as a well-mixed unit in which a given compartment is uniformly labeled. The chosen segment length must be short enough that this approximation is reasonable. To represent NH_4^+ spiraling with distance, our selected segment was a small fraction (<20%) of the expected uptake distance. The Kuparuk River calibration links 50 stream segments, each 100 m long, for a total modeled reach of 5 km. Therefore, stocks are specified as g N/100-m segment and fluxes as g N 100-m segment^{-1} d^{-1}. For comparison with field data and literature, our calibration values are shown as stocks per m^2 in the tables. Fluxes between volume compartments are also given on an areal basis to achieve mass balance (Appendix).

Two other features of SISTM are the ability to vary advective N fluxes into the reach over time and the incorporation of lateral N inputs over distance. Because we added tracers at a constant rate, changes in discharge or nutrient concentration altered enrichment in the target compartment. SISTM incorporates this variation by drawing advection information from a file of daily N fluxes. External fluxes can enter each segment via lateral inputs. For N compartments with lateral inputs, each segment receives the same amount of unlabeled N estimated from lateral input rates and nutrient concentration. As with upstream inputs, these inputs can vary with time.

Model calibration

Field measurements.—Stocks and fluxes for a given calibration were derived from field measurements, literature estimates, or reasonable estimates constrained by known fluxes. The initial calibration used data from before 1991 and literature estimates from similar streams. Later calibrations incorporated field measurements made during the 1991 field season. In this section we discuss how we estimated N stocks and major N fluxes.

The Kuparuk River has been intensively studied since 1983, when a PO_4^{3-} fertilization experiment began (Peterson et al. 1993). The measurements and tracer addition discussed in this paper involved the unfertilized reference reach of the Kuparuk starting roughly 1.6 km upstream of the fertilized reach. The Kuparuk is composed of ~50% each of pool and riffle habitat that is fairly representative of 100-m segments. Therefore, we averaged pool and riffle biomass and flux estimates for an overall segment average. The average volume and area of each 100-m segment were 680 m^3 and 1700 m^2, respectively, based on a mean stream width of 17 m and depth of 0.4 m.

Nitrogen stocks and advective inputs of DIN, DON, and PON were derived from mean summer concentration estimates: NO_3^--N and NH_4^+-N were measured using an Alpkem autoanaly-

TABLE 1. Estimates of N stocks from field measurements in the Kuparuk River during summer of 1991. Because N was not always directly measured, conversion factors and assumptions used to derive N stock from field measures are listed. DON = dissolved organic N, PON = particulate organic N, Chl = total chlorophyll, DM = dry mass, WM = wet mass, ind. = individual.

Compartment	Field measure and conversion factors	Estimate (mg N/m²)
NO_3^-	11.2 μg/L * 0.4 m depth	4.5
NH_4^+	2.8 μg/L * 0.4 m depth	1.1
DON	250 μg/L * 0.4 m depth	100
PON	14 μg/L * 0.4 m depth	5.6
Benthic detritus	28 g C/m² * C:N = 13	2180
Moss	19.1 g DM/m² * 2.3% N	440
Filamentous algae	0.47g DM/m² * C:DM = 0.45 * C:N = 7	30
Diatoms	1.6 μg Chl/cm² * C:Chl = 50 * C:N = 7	120
Epilithic detritus	34 μg N/cm² − diatom mass	240
Insects	C:DM = 0.45, C:N = 5, habitat = 35%	
Brachycentrus	65/m² * 1.25 mg DM/ind.	2.5
Prosimulium	5400/m² * 0.19 mg DM/ind.	32
Baetis	1400/m² * 0.11 mg DM/ind.	5
Orthocladius	450/m² * 0.35 mg DM/ind.	5
Other chironomids	1840/m² * 0.066 mg DM/ind.	3.8
Grayling	DM:WM = 0.2, C:DM = 0.45, C:N = 5	
Adults	0.45 ind./m² * 500 g WM/ind.	29
Young-of-the-year	10 ind./m² * 0.31 g WM/ind. * habitat = 50% (pools only)	12

zer, DON by subtracting DIN from TDN measured using an Alpkem following persulfate digestion, and PON using a Perkin-Elmer CHN analyzer. Stocks of these compartments were calculated from concentration and water volume in the 100-m segment. Discharge was determined from stage height recorded continuously during the experiment and stage vs discharge regressions developed in 1991. Advective inputs were calculated from concentration and discharge.

Nitrogen stocks of epilithon were determined from CHN analysis of rock scrubbings of known area. For the final calibration (Update 3), epilithon was divided into diatom-N and epilithic detrital-N compartments. Nitrogen stocks in each component were calculated from total N in epilithon minus an estimate of diatom N (Table 1), based on total chlorophyll (Chl) estimates (Golterman and Clymo 1969) and assuming a C:Chl mass ratio of 50:1 (Eppley 1972) and C:N mass ratio of 7:1, slightly greater than the 5.7:1 mass ratio of Redfield (1958). Epilithon was measured only in riffles, but was assumed to be the same in pools. Moss N stocks were determined from dry masses and CHN analysis. Moss occurred only in riffles, and the reported estimate incorporates the lack of moss in pools. Insect stocks were determined in riffles from abundance estimates and length measurements (A. E. Hershey, unpublished data) and converted to dry masses using length–mass regressions (Smock 1980). To convert to N content, we assumed a C:dry mass ratio of 0.45 and a C:N ratio of 5 (Table 1), both based on measurements of cladoceran and copepod invertebrates (Sterner and Hessen 1994). We assumed 35% of the total stream surface area was colonized by insects because pools have very low insect densities and stream edges are marginal insect habitat. Estimates of adult and young-of-year grayling N stocks were determined from numbers, mean wet masses (L. A. Deegan, unpublished data), dry:wet mass = 0.2, C:dry mass = 0.45, and C:N = 5 (Table 1). Benthic detritus was not measured in 1991; instead we used the estimate of C stocks from Peterson et al. (1986) and assumed a C:N ratio of 13 (B. J. Peterson, unpublished data). Filamentous algal N stocks were estimated from mass vs % cover regressions. We used a 1% cover estimate and assumed the same C:N ratio as epilithic diatoms.

The set of possible input and output fluxes for each type of compartment is listed in Table 2.

TABLE 2. Difference equations for parameterization of N fluxes in the calibration for the Kuparuk River. All units are in mass N area^{-1} time^{-1}. Change in total N for each time unit (dN/dt) was assumed to be 0 for all equations except dissolved organic N (DON), particulate organic N (PON), and detritus, all of which accumulated N to keep downstream flux of dissolved inorganic nitrogen (DIN) constant in calibrations that included lateral inputs.

1) Primary producers dN/dt = (NH_4^+ uptake + NO_3^- uptake) − (DON leaching + PON sloughing + consumption by insects + mortality to detritus)
2) Insects dN/dt = consumption − (waste NH_4^+ + waste PON + predation + mortality)
3) Fish dN/dt = consumption − (waste NH_4^+ + waste PON + mortality)
4) PON dN/dt = (resuspension from detritus + primary producer sloughing + waste inputs) − (settling to detritus + breakdown to DON + filter feeding)
5) DON dN/dt = (leachate from primary producers + PON breakdown + leachate from detritus) − (detrital and epilithic heterotrophic uptake)
6) NO_3^- dN/dt = (nitrification of water column NH_4^+ + nitrification of benthic N + lateral inputs) − primary producer uptake
7) NH_4^+ dN/dt = (waste inputs + remineralization of detritus + lateral inputs) − (primary producer uptake + water column nitrification + heterotrophic uptake)
8) Detritus dN/dt = (heterotrophic NH_4^+ uptake + heterotrophic DON uptake + PON settling + primary producer mortality + insect mortality + fish mortality) − (remineralization of NH_4^+ + benthic nitrification + resuspension + insect consumption + DON leaching)

In general, we assumed inputs equaled outputs (dN/dt = 0) with the exceptions noted below. Nitrogen uptake by primary producers was derived from primary production rates measured in the field. Primary production of epilithon and mosses was estimated in 1991 and 1995, respectively, as the mean of pool and riffle measurements of O_2 change in chambers (Bowden et al. 1992, Arscott 1997). We assumed primary production rates of mosses in the reference reach in 1995 were the same as in 1991. To derive N uptake, we assumed a C:N ratio of 7:1 for epilithon and 25:1 for moss (Table 3). Filamentous alga production was not measured in the Kuparuk. However, we used measurements made during a fertilization (N and P) experiment at nearby Oksrukuyuk Creek, Alaska (D. B. Arscott, University of New Hampshire, personal communication), which were then scaled down based on the much lower % cover in the reference zone of the Kuparuk. As with epilithon, we derived N uptake assuming a C:N ratio of 7:1. Because primary production was estimated under optimal light conditions, we scaled all primary production estimates (and N uptake) by 2/3 to account for reduced light conditions caused by overcast skies and nights when the sun was close to the horizon. The sun did not set during the experiment.

We assumed a constant stock of primary producers during the addition period, so inputs balanced outputs. Epilithic uptake was balanced by outputs to DON (10% of N inputs), grazing by insects (flux determined below), and the remainder by sloughing to PON (Table 2). Outputs from filamentous algae and moss were assumed to be 10% to DON and the rest to benthic detritus.

Nitrogen-fluxes to insects were estimated from mean mass change for each taxon between measurements taken early and late in the experiment. Biomass increment was divided by the number of days between sampling, assuming constant growth. Growth rates were measured for *Brachycentrus, Prosimulium,* and *Baetis* (Table 3). Growth rates for *Orthocladius* and other chironomids were approximated using the *Prosimulium* rate. The measured change in mass was assumed to represent 1/3 of total N intake during the addition, with the remainder attri-

TABLE 3. Estimates of N fluxes from field measurements in the Kuparuk River during the summer of 1991. Because N was not always directly measured, conversion factors and assumptions used to derive N flux from field measures are listed. Conversion factors applied to all compartments of a given type (e.g., primary producer, insect, etc.) are listed on the 1st line for each type. See the Appendix for the full matrix of fluxes used for the final model calibration. DM = dry mass, WM = wet mass, ind. = individual.

N flux	Field measure and conversion factors	Estimate (mg N m^{-2} d^{-1})
Primary producer uptake	N uptake reduced 2/3 to account for periods of reduced light	
Diatoms	41.5 mg O_2 m^{-2} h^{-1} * mg C:mg O_2 = 0.313[a] * C:N = 7	30
Moss	0.109 mg C g DM^{-1} h^{-1} * 19.12 g DM/m^2 * C:N = 25	1.4
Insect N uptake	assumed net assimilation = 1/3 of uptake, habitat = 35%	
Brachycentrus	65/m^2 * 0.0007 mg N $ind.^{-1}$ d^{-1}	0.05
Prosimulium	5400/m^2 * 0.00068 mg N $ind.^{-1}$ d^{-1}	4.0
Baetis	1400/m^2 * 0.00049 mg N $ind.^{-1}$ d^{-1}	0.7
Orthocladius	assumed same turnover time as *Prosimulium*	0.7
Other chironomids	1840/m^2 * 0.00068 mg N $ind.^{-1}$ d^{-1}	1.4
Grayling N uptake	DM:WM = 0.2, C:DM = 0.45, C:N = 5, assimilation = 1/3	
Adult	0.45 ind./100 m^2 * 1.3 g WM/d	0.2
Young-of-the-year	10 ind./m^2 * 0.31 g WM/ind. * habitat = 50% (pools only)	1.0
Seepage NH_4^+	336 μg/L * 1% water dilution/km ÷ 14 m width	12.9
Seepage NO_3^-	112 μg/L * 1% water dilution/km ÷ 14 m width	4.1

[a] Derived from a photosynthetic quotient (O_2:C molar ratio) of 1.2

buted to waste products (as NH_4^+ and PON), predation, or natural mortality. Thus, total N flux to each insect was estimated as growth uptake multiplied by 3. Insects were modeled at constant N stocks, with natural mortality (to benthic detritus) and/or predation balancing the field growth estimate (Table 2, Appendix). Daily N flux to grayling was also determined from changes in mean mass measured early and late in the addition, and by assuming constant growth.

We assumed *Baetis* grazed epilithon (Hershey et al. 1993), *Orthocladius* grazed a pure culture of diatoms located on its feeding tube (Hershey et al. 1988), *Prosimulium* and *Brachycentrus* fed on PON (Hershey and Hiltner 1988), and chironomids fed both on benthic detritus and epilithon (Appendix). The assumption that *Orthocladius* fed on pure diatoms was important because we also assumed the observed labeling in *Orthocladius* was equivalent at equilibrium to the labeling of diatoms in the epilithic biofilm, which we could not directly measure. That is, we assumed *Orthocladius* was a sampler of the $\delta^{15}N$ value for the diatom component of epilithon.

Lateral inputs of NO_3^- and NH_4^+ were derived from an estimate of water input rate based on watershed area and water yield from precipitation across the watershed. This estimate yielded a 1% increase in discharge per km of stream channel. Mean concentrations of NO_3^- and NH_4^+ in seepage water were 112 μg/L and 336 μg/L, respectively, as measured in streamside lysimeters (M. C. Miller, unpublished data).

Nitrification rates were estimated from the increase in NO_3^- concentrations downstream of a fertilizer addition of NH_4^+-N (Peterson et al. 1993). In 1986, NH_4^+ was added to the P-fertilized reach of the Kuparuk, raising its concentrations to 330 μg/L, which declined to 120 μg/L over 2 km. Nitrate concentrations simultaneously increased from 56 to 110 μg/L. The rate of nitrification was derived as a % of total NH_4^+ disappearance converted to NO_3^-, or ~ 30% over 2 km (Appendix). Because this estimate was derived from an enrichment study, it should be viewed as a maximum nitrification rate at ambient NH_4^+ levels.

The distance-specific rate of suspended PON deposition to the stream bottom was assumed to be 0.002/m. This rate is within the range Cushing et al. (1993) reported for similar-sized streams in Idaho. The daily flux of PON to the

stream bottom was calculated from the deposition rate and the median advective influx during the addition. PON resuspension was assumed to be the difference between PON settling and PON inputs from sloughing of algae and waste excretion from insects and fish (Table 2, Appendix). The model is zero-order, so the PON flux remains constant over time despite variation in discharge for the later calibrations.

There were numerous other fluxes for which we had no data, including heterotrophic uptake of DIN and remineralization of DIN from detritus. The fluxes estimated above provided constraints for these unknown fluxes, using the assumption of steady state for most N stocks. For example, we used the large detritus pool to balance uptake or inputs of NH_4^+ and NO_3^-. In calibrations that included lateral inputs (Update 2 and later), imbalances were allowed in the benthic detritus compartment as well as in DON and PON. Thus, the net result of lateral inputs was either conversion to DON or PON, or retention by benthic detritus. Although we have no measurements to verify these imbalances, they were necessary to account for N load from lateral inputs while satisfying the field observation of no change in NH_4^+ and NO_3^- concentrations over distance throughout the study reach during the experiment. The accumulation of benthic detrital N during summer seems reasonable because organic matter levels often increased during low discharge, and were reset during high discharge (Meyer and Likens 1979). We did not have a high-discharge event in 1991 until just prior to the end of the addition.

Calibration series.—A procedure for using SISTM in conjunction with tracer additions in streams was tested in a series of 4 calibrations (Fig. 2). Each calibration reflected additional knowledge accrued during these studies. We compared the modeled $\delta^{15}N$ values with observed $\delta^{15}N$ values for each calibration. The a priori calibration modeled the system as simply as possible using only data available prior to the experiment, and where data were unavailable included numerous assumptions. This calibration used mean summer discharge, nutrient concentration, primary production, and biomass of various compartments calculated from data collected prior to 1991 (Table 4). It assumed no lateral N inputs, and all N uptake by primary producers and heterotrophs was as NH_4^+. The latter assumption, a prominent feature in the a priori

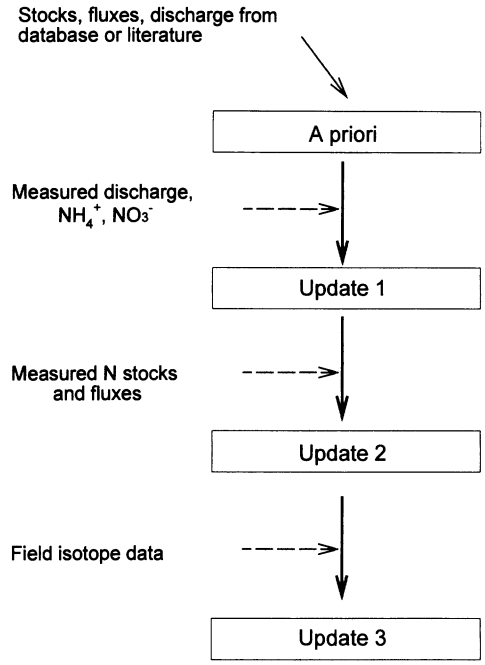

FIG. 2. Sequence of calibrations reflecting the increased information during a tracer addition.

calibration, was based on the river usually being P limited with excess DIN (Peterson et al. 1983). Nitrogen:phosphorus (>10:1) is relatively high in the Kuparuk reference section, so we expected more reactive NH_4^+ would be preferentially taken up over relatively unreactive NO_3^-. Our assumptions reflected the limits of available knowledge for our stream at the start of the experiment.

Updates 1 and 2 incorporated field-measured stocks and fluxes while retaining the remainder of the a priori calibration (Table 4). Update 1 used the same a priori stocks and fluxes, but included measured variables that affected tracer dilution, such as discharge and NH_4^+ concentration. Update 2 incorporated more detailed measurements of stocks and fluxes during the addition period, but no stable isotope tracer data. In this calibration, some unmeasured fluxes were modified as necessary to keep compartments in balance, or allow for processing of lateral inputs. Update 3 demonstrated how insights from the field isotope data could help account for differences between observed and predicted $\delta^{15}N$ values (Table 4). This update included 2 model runs that sequentially incorporated new findings from the isotope data.

TABLE 4. Key variables updated in the sequence of model calibrations using field data from the 1991 experiment. Bold values indicate model calibrations in which the 1991 field data were included. Other unmeasured fluxes were also changed in each calibration to balance with updated flux measurements but are not included here.

Parameter	A priori	Update 1	Update 2	Update 3
Discharge (m^3/s)	2.15	**variable (median = 0.75)**	**variable**	**variable**
NH_4^+ (μg N/L)	15.4	**2.8**	**2.8**	**2.8**
Lateral inputs (mg N m^{-2} d^{-1})				
NH_4^+	0	0	**12.9**	**12.9**
NO_3^-	0	0	**4.1**	**4.1**
N stocks (mg N/m^2)				
Moss	30	30	**440**	**440**
Epilithon	305	305	**360**	**360**
Diatoms	0	0	0	**120**
Epilithic detritus	0	0	0	**240**
Prosimulium	65	65	**32**	**32**
Baetis	4	4	**5**	**5**
Orthocladius	2	2	**5**	**5**
Epilithic N uptake (mg N m^{-2} d^{-1})	19	19	**30**	**30**
N preference (% NH_4^+:NO_3^-)				
Filamentous algae	100:0	100:0	100:0	**80:20**
Epilithon/diatoms	100:0	100:0	100:0	**45:55**
Moss	100:0	100:0	100:0	**20:80**

These runs included NO_3^- and NH_4^+ uptake by each of the 3 primary producer compartments, and the division of bulk epilithon into diatom and epilithic detritus compartments. For the complete set of fluxes in the final calibration see the Appendix.

Tracer addition

The details of the whole-stream tracer addition were described in Peterson et al. (1997). To summarize, stable isotope tracer, ^{15}N-NH_4Cl (10% ^{15}N), was added to an unfertilized reach of the Kuparuk River continuously over a 6-wk period at a rate of 0.89 g/d of ^{15}N. This rate of addition increased NH_4^+-N concentration in the stream <1% above background NH_4^+ concentration. We therefore assumed the ^{15}N-NH_4^+ was a true tracer for NH_4^+ that followed pathways reflecting N dynamics at ambient levels. The continuous addition was accomplished with a peristaltic pump located at a narrowly focused riffle where mixing was rapid. The pump reliably delivered the target amount of ^{15}N throughout the addition. Median daily enrichment of NH_4^+ was roughly 1100 ‰ at the point of addition. This increase in $\delta^{15}N$ was sufficiently large relative to the natural abundance of $\delta^{15}N$ that an easily measured and unambiguous signal developed throughout the riverine food web.

Weekly samples of biota determined the flow of tracer N through the food web over distance and time. Stations were located 0.08, 0.18, 0.68, and 0.85 km downstream of the addition site with additional stations at 1.6, 3, and 4 km late in the addition. Data from the 0.08 km station were erratic because of incomplete cross-channel mixing, and were not used for comparison with model-predicted values. Compartments sampled weekly were filamentous algae, epilithon, *Orthocladius*, *Baetis*, and *Prosimulium*. Moss, adult grayling, and young-of-year grayling were collected late in the experiment. Samples were analyzed at the Ecosystems Center in Woods Hole for $\delta^{15}N$ value with a Finnegan Delta-S mass spectrometer. Results are presented as $\delta^{15}N$ values defined as $\delta^{15}N = (R_{sample}/R_{standard} - 1) * 1000$ where $R = {}^{15}N:{}^{14}N$ and the N isotope ratio standard is air.

Comparison of expected and observed tracer distributions

We assessed how well the model described overall NH_4^+ dynamics by determining uptake length of NH_4^+ (S_w), a measure of the average distance a nutrient molecule travels before being taken up (Newbold et al. 1981). Because we could not measure $\delta^{15}N$-NH_4^+ directly, we calculated S_w using the downstream decline of *Orthocladius* $\delta^{15}N$ as a surrogate. To calculate S_w we used $\delta^{15}N$ of *Orthocladius* at stations up to 1.6 km downstream of the drip site ($n = 4$) on day 35 of the addition. Del values were natural-log transformed to obtain the slope of the decline, the inverse of which is S_w (Stream Solute Workshop 1990). Predicted S_w was similarly calculated from the results of each model calibration. Use of *Orthocladius*, a diatom grazer, to estimate S_w is valid because the downstream decline in its $\delta^{15}N$ (and its diatom food source) should be proportional to the decline of $\delta^{15}N$-NH_4^+ (but see exception below). Because *Orthocladius* creates feeding tubes attached to rocks, we assumed there was no downstream drift skewing the isotope distribution. We made the comparison late in the addition (day 35) to incorporate dynamics throughout the addition period.

Normally, S_w is calculated using the downstream decline in concentration of solute or tracer. Measurement of stable isotope tracer is in the form of a ratio of ^{15}N to ^{14}N ($\delta^{15}N$). The δ ratio can be used in place of tracer concentration in this calculation only if ^{14}N is assumed to be constant over distance. We made this assumption because no longitudinal gradients of DIN have been observed in the Kuparuk reference reach.

Complications can arise when calculating NH_4^+-S_w from long-term tracer additions, and when using the biota as a surrogate for NH_4^+-S_w. The S_w calculation has been previously applied only during short-term tracer or solute additions where negligible regeneration is assumed (Newbold et al. 1983a, Mulholland et al. 1985). In our long-term addition, ^{15}N-NH_4^+ regeneration was likely, causing tracer levels to be higher downstream than expected from NH_4^+ disappearance alone, especially late in the experiment. Measured S_w would then exceed the true S_w. Elevated tracer levels were observed downstream, but because our model-predicted S_w also incorporated ^{15}N regeneration, the comparison of observed and predicted S_w was valid.

Using the biota to calculate NH_4^+-S_w potentially involved a 2nd complication. In streams where nitrification rates are high, ^{15}N-NH_4^+ will be transformed to ^{15}N-NO_3^-. As a result, $\delta^{15}N$-NO_3^- is likely to increase downstream, where $\delta^{15}N$-NH_4^+ is reduced because of uptake and nitrification. Primary producers that assimilate NO_3^- as well as NH_4^+ will have a higher downstream $\delta^{15}N$ value than if only NH_4^+ was taken up. In such a scenario, S_w determined using biota will be higher than the true NH_4^+-S_w. We could not measure the $\delta^{15}N$ values of NO_3^- to assess its effect on the S_w calculation. The potential complication was somewhat reduced by using sampling stations where $\delta^{15}N$-NH_4^+ was expected to be comparable to or higher than $\delta^{15}N$-NO_3^- (i.e., only stations from 0.18 to 1.6 km were used to calculate S_w). Although NH_4^+-S_w as reported in this paper was possibly an overestimate, we felt a comparison of predicted vs observed S_w using the biota was still a useful indicator of whether a model calibration adequately represented field dynamics.

We also assessed how well food web dynamics were described in each calibration by comparing the ratio of predicted and observed $\delta^{15}N$ values of *Baetis* and *Prosimulium* at individual stations throughout the addition. A predicted/observed $\delta^{15}N$ of 1 meant exact correspondence. The $\delta^{15}N$ values of these 2 insect taxa reflected different aspects of the N cycle, with *Baetis* more connected to epilithic primary production and *Prosimulium* to PON dynamics.

Results

A priori: initial calibration

Predicted $\delta^{15}N$ values from the a priori calibration corresponded poorly with observed data. Predicted $\delta^{15}N$ values for *Orthocladius*, *Baetis*, and *Prosimulium* were much lower than observed $\delta^{15}N$ in segments close to the dripper (Figs 3A,B, 4A, 5A) and higher than observed further from the dripper (Fig. 3B). As a result, predicted S_w on day 35 as determined from *Orthocladius* was 5.3 km, whereas observed S_w was 0.84 km (Table 5).

Predicted $\delta^{15}N$ values were low because the added tracer was diluted by higher advective N input than observed in the field. The a priori calibration used a pre-1991 summer mean discharge and NH_4^+ concentration of 2.15 m^3/s

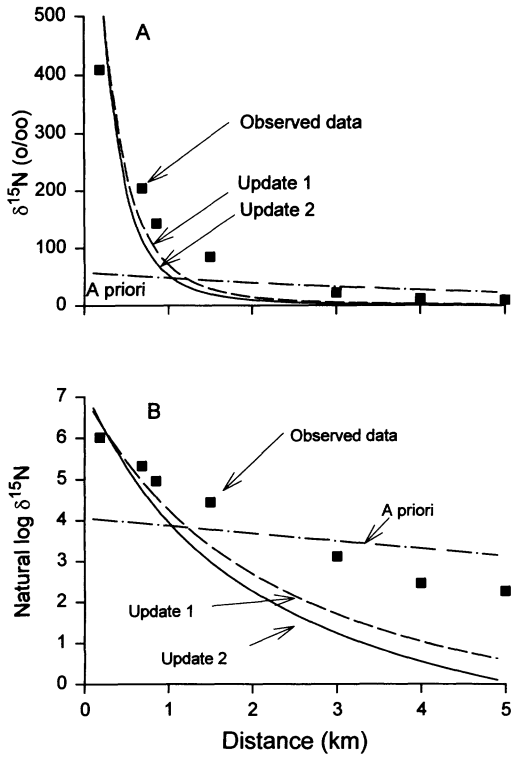

FIG. 3. Comparison of observed and predicted decline in (A) untransformed $\delta^{15}N$ and (B) natural-log-transformed $\delta^{15}N$ over distance using the first 3 model calibrations (A priori, Update 1, Update 2). Data are for *Orthocladius* on day 35 of the tracer addition.

and 15.4 μg/L, respectively, which were both much higher than values monitored during the experiment. Actual discharge was low and relatively stable (median = 0.75 m^3/s) and NH_4^+ concentration was low (summer mean = 2.8 μg/L). The large advective inputs using pre-1991 data resulted in a much longer S_w for the given rate of uptake. Because of tracer dilution caused by high advective N inputs, testing whether a priori fluxes would distribute the tracer adequately over time and distance was not possible.

Update 1: measured discharge and nutrient concentration

We next incorporated measured daily discharge and mean concentration of NH_4^+ during the experiment (Table 4), which allowed the model to start with an accurate estimate of daily ^{15}N-NH_4^+ enrichment at the dripper (Fig. 6). The

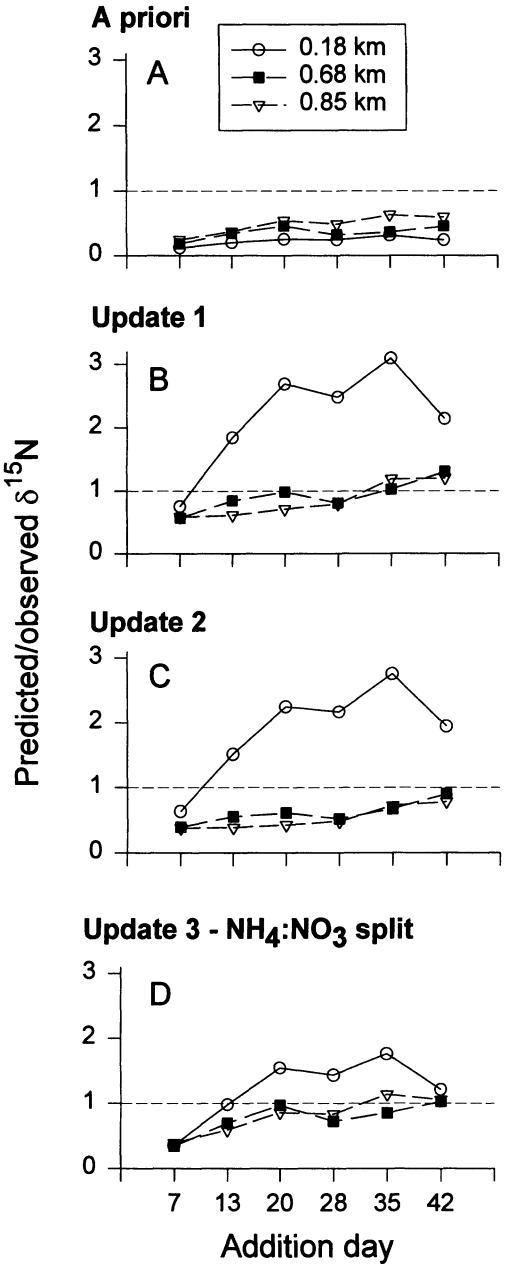

FIG. 4. The ratio of predicted and observed $\delta^{15}N$ of *Baetis* using calibration data. A.—Derived using data from years prior to 1991 (A priori). B.—Updated for measured daily discharge and mean nutrient concentration during the experiment (Update 1). C.—Updated with all stocks and fluxes measured during the 1991 experiment (Update 2). D.—After using the isotope data to parameterize N preference and split the epilithon compartment. A ratio of 1 means predicted values equal observed values. Data are for *Baetis* at 0.18, 0.68, and 0.85 km downstream from the addition site over the 42-d addition period.

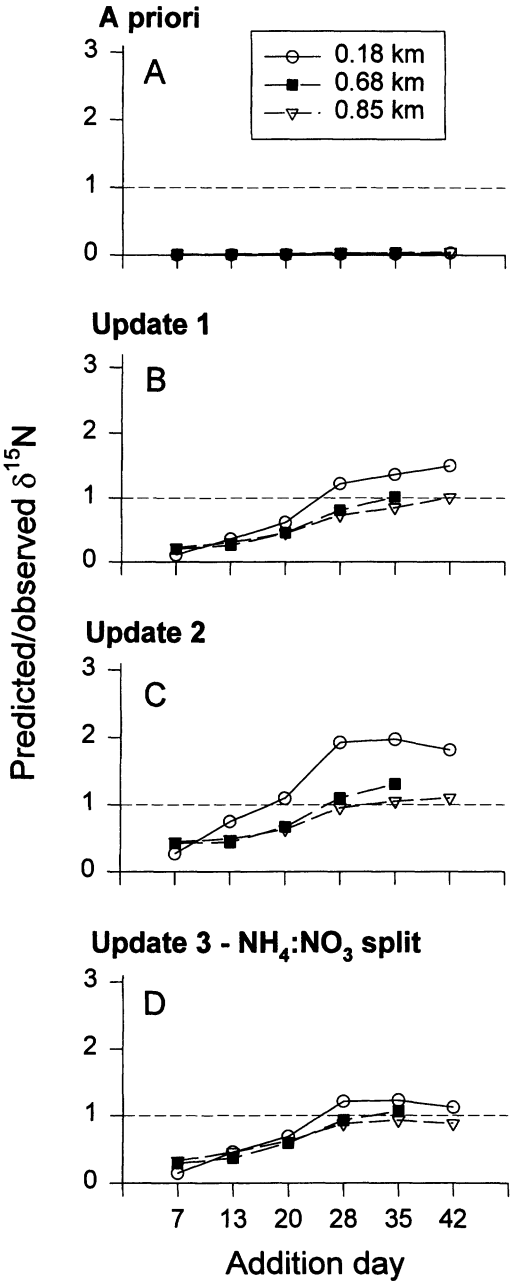

FIG. 5. The ratio of predicted to observed $\delta^{15}N$ of *Prosimulium* using (A) the A priori calibration, (B) Update 1, (C) Update 2, and (D) Update 3. A ratio of 1 means predicted values equal observed values. Data are for *Prosimulium* at 0.18, 0.68, and 0.85 km downstream from the addition site over the 42-d addition period.

TABLE 5. Uptake length (S_w) calculated using day 35 *Orthocladius* predicted by each model calibration and by the field data. Only data points up to 1.6 km were used to minimize the potential impact of nitrification and ^{15}N regeneration on estimates using the biota.

Model Calibration	S_w (km)
A priori	5.30
Update 1	0.44
Update 2	0.39
Update 3 (NO_3:NH_4 split)	0.67
Update 3 (Epilithon split)	0.71
Observed	0.84

results were much improved over the a priori calibration, but large differences remained in the rate of $\delta^{15}N$ decline downstream and between observed and predicted $\delta^{15}N$ in biota. Predicted S_w was now 0.44 km, compared with the observed S_w of 0.84 km (Fig. 3B, Table 5). Possibly the modeled advective NH_4^+ influx was now too low, which would elevate $\delta^{15}N$ values close to the dripper and shorten S_w. NH_4^+ is extremely difficult to measure at low concentra-

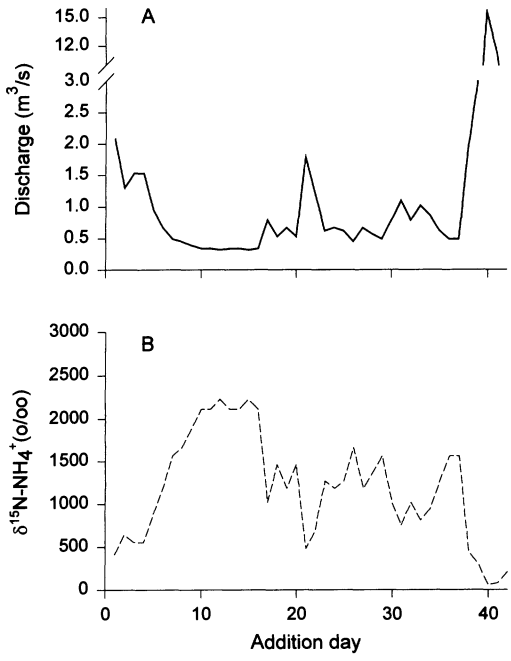

FIG. 6. (A) Mean daily discharge (m^3/s) and (B) estimated daily $\delta^{15}NH_4^+$ enrichment (o/oo) at the addition site during the 42-d addition period.

tion (Aminot et al. 1997) and the actual concentration could possibly have been double the 2.8 μg/L we included in this calibration. We assume for the remainder of this paper that NH_4^+ concentration and estimated NH_4^+ enrichment were correct. If total advective NH_4^+ influx was reasonable, then the short predicted vs observed S_w resulted from overestimating NH_4^+ removal by benthic processes.

The correspondence between predicted and observed $\delta^{15}N$ for *Baetis* was somewhat improved over the a priori calibration (Fig. 4B). The pattern reflected the short NH_4^+-S_w in this calibration, resulting in overestimates close to the dripper (0.18 km station), but reasonable correspondence downstream at 0.68 and 0.85 km. The correspondence occurred at these 2 stations because the decay function of the predicted and observed $\delta^{15}N$-NH_4^+ (as inferred from the biota, Fig. 3B) nearly cross. Further downstream, predicted $\delta^{15}N$ values were increasingly underestimated.

The pattern of predicted/observed $\delta^{15}N$ for *Prosimulium* was also improved over the a priori calibration (Fig. 5B). Predicted/observed $\delta^{15}N$ was low for all 3 stations early in the addition (Figs 5B, 7A), but improved steadily as the experiment continued (Figs 5B, 7B). Changes in the predicted/observed $\delta^{15}N$ over time (Fig. 5B) could result from longer *Prosimulium* turnover times in the calibration than in the field. The relatively good correspondence late in the addition was surprising. In our calibrations, *Prosimulium* fed on PON labeled mainly via sloughing epilithon. Both PON and *Prosimulium* $\delta^{15}N$ should reach similar peaks somewhere downstream of the maximum epilithon label. The size of the peak is a factor of the magnitude and distribution of source (epilithon) label, the relative amount of sloughing and advective PON influx, and the rate of PON settling. The epilithon source in this calibration was too highly labeled close to the addition point and the ^{15}N decay rate of epilithon was too rapid (as inferred from *Orthocladius;* Fig. 3B, Table 5). Thus the relatively good correspondence between predicted and observed *Prosimulium* $\delta^{15}N$ late in the addition was achieved despite erroneous source pool ^{15}N distribution.

Compared with the a priori calibration, Update 1 resulted in predicted $\delta^{15}N$ patterns in the biota comparable to observed $\delta^{15}N$ because total N flux, as determined by discharge, is a dominant variable in tracer additions to streams. However, major discrepancies remained, indicating that some of our original flux terms were incorrect.

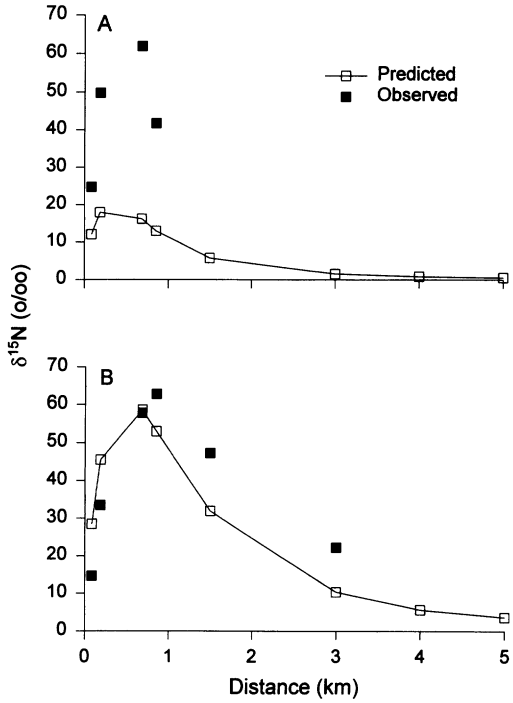

FIG. 7. Observed and predicted (Update 1) $\delta^{15}N$ versus distance for *Prosimulium* on (A) day 14 and (B) day 35.

Update 2: field-measured stocks and fluxes

Update 2 further refined the model calibration by including several stocks and fluxes measured during the experiment. These refinements included a much higher estimate of moss biomass, higher primary production of epilithic algae, improved insect stock and growth data, and an estimate of NH_4^+ and NO_3^- lateral inputs (Table 4). Predicted S_w declined to 0.39 km in Update 2 compared to 0.44 km in Update 1 and 0.84 km observed (Fig. 3B, Table 5). The S_w decline in Update 2 was caused by the increased total NH_4^+ uptake by the stream bottom that resulted from the higher estimate of epilithic primary production and higher moss biomass (Table 4).

The decline in S_w was minor (11%) compared to increased NH_4^+ uptake (33%) because of the

counterbalancing effect of lateral inputs. Lateral inputs via seepage of NH_4^+ and NO_3^- from tundra soils were considered to be uniform along the entire reach. Their inclusion enhanced total N flux into each stream segment, increasing total NH_4^+ flux by 12%. Increased NH_4^+ influx would lengthen S_w, but increased NH_4^+ uptake would shorten it. The net effect was the 11% decline in S_w.

Lateral inputs added to each segment can be a significant N supplement to the stream. Although seepage waters contain much higher DIN concentrations than stream water, we observed no DIN increase with distance downstream. As a result, lateral inputs must be balanced by retention, denitrification, or transformation to compartments such as DON or PON subsequently transported downstream. This calibration balanced lateral inputs by accumulation of benthic detritus over time (0.7% of initial N stock per day) and by transformation to DON (0.6% increase over 5 km) or PON (2% increase over 5 km). We have no field measurement confirmations of these imbalances. These fates were selected because the large N stocks in these compartments could absorb a small steady accumulation of N with time (detritus) or distance (DON and PON) with little impact on N stocks or compartment $\delta^{15}N$ values. The actual fate of N lateral inputs requires further study.

The large increase in moss N stock, from an a priori estimate of 30 mg N/m^2 (unmeasured estimate) to a measured 440 mg N/m^2 (Table 4), had little impact on overall N dynamics. This large change had less impact on NH_4^+ uptake than one might expect because of low measured primary production rate and hence slow N uptake by the moss, *Schistidium* (Arscott 1997). Consequently, even after revising the stock estimate, moss uptake composed only 5–6% of total NH_4^+ uptake.

Incorporation of field measurements in Update 2 did not greatly affect the fit between predicted and observed $\delta^{15}N$ values for *Baetis* (Fig. 4C). The higher predicted/observed $\delta^{15}N$ for *Prosimulium* (Fig. 5C) compared with Update 1 (Fig. 5B) occurred primarily because sloughing of epilithon to PON was increased by 50% to balance higher epilithic primary production. This increase resulted in higher enrichments of the PON and *Prosimulium* compartments.

Because incorporation of the measured stocks and fluxes did not improve our ability to predict tracer location, some other aspect of our model calibration was incorrect. Lack of resources or technology to measure every flux meant that certain fluxes remained assumptions or approximations. To improve these estimates, we next used the isotope data itself to develop a model calibration that more clearly reflected N-cycle structure in situ.

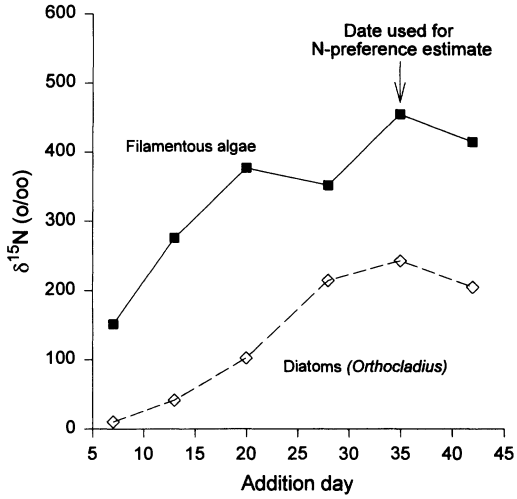

FIG. 8. Increase of $\delta^{15}N$ in filamentous algae and diatoms (using *Orthocladius* as a surrogate) versus time in the Kuparuk River during the 1991 ^{15}N addition. Day 35 values are assumed to represent completely labeled compartments.

Update 3: using the field isotope data

NH_4^+ vs NO_3^- uptake.—Our 1st problem was the shorter predicted than observed NH_4^+-S_w (i.e., removal of NH_4^+ predicted by the model was too high). If distribution of $\delta^{15}N$-NH_4^+ in the model was incorrect, then predicted transfer to recipient compartments was also erroneous. Based on the contrasting observed $\delta^{15}N$ values for filamentous green algae, mosses, and *Orthocladius* at equilibrium, we hypothesized that NO_3^- was also taken up. To assess this, we derived the N preference (NH_4^+ and NO_3^-) for each primary producer (diatoms, filamentous algae, moss) from the field isotope data.

By day 35, $\delta^{15}N$ values had stabilized in filamentous algae and diatoms (estimated using *Orthocladius*), indicating maximum enrichment (Fig. 8). To partition NH_4^+ vs NO_3^- uptake, we

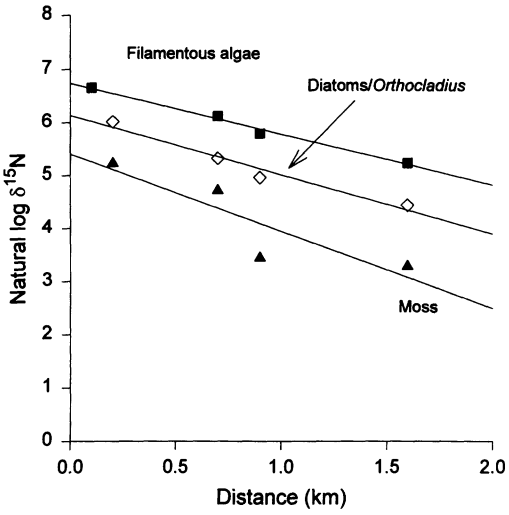

FIG. 9. Observed natural-log-transformed $\delta^{15}N$ values for the 3 primary producers late in the experiment. The intercept from regressions of each primary producer represents the $\delta^{15}N$ values at the addition site.

plotted the natural-log-transformed data vs distance for each primary producer (Fig. 9). The intercept was used to calculate the $\delta^{15}N$ of each primary producer at the drip site. We then compared the calculated $\delta^{15}N$ value for each primary producer to the median estimated $\delta^{15}N$-NH_4^+ value derived from the ^{15}N drip rate, N concentration, and mean discharge during 1 N turnover time of each compartment. The ratio of primary producer $\delta^{15}N$ at this equilibrium stage and the estimated $\delta^{15}N$-NH_4^+ was used to indicate DIN preference.

Based on these calculations we partitioned uptake between NH_4^+ and NO_3^- at ratios of 80:20 for filamentous algae, 45:55 for diatoms and 20:80 for mosses (Table 6). Total N uptake for each primary producer was left unaltered. The result was a large decrease in ammonium uptake from 45 to 26 mg N m^{-2} d^{-1} and an increase in NO_3^- uptake by primary producers from 0 to 19 mg N m^{-2} d^{-1}. The reapportionment alleviated the need to include some questionable fluxes such as the high uptake of NO_3^- by benthic detritus. We had invoked this flux to keep NO_3^- concentrations constant along the reach despite lateral inputs and nitrification. The model calibration now predicted an S_w of 0.67 km, much closer to the observed 0.84 km (Table 5), and showed good correspondence between predicted and observed $\delta^{15}N$ values along the entire reach (Fig. 10A). We note that the model indicated that the predicted S_w estimates using biota $\delta^{15}N$ values were ~35% higher than the true NH_4^+-S_w estimate (using $\delta^{15}NH_4^+$) because of the skewing effect of nitrification and subsequent $^{15}NO_3^-$ uptake by biota at downstream stations.

Predicted $\delta^{15}N$ values for *Baetis* were brought closer to observed values (Fig. 4D), whereas previously they were much higher at 0.18 km and lower at 0.68 and 0.85 km (Fig. 4C). Elevated predicted/observed $\delta^{15}N$ close to the dripper in Updates 1 and 2 resulted from higher than observed enrichment of the *Baetis* food source (because of 100% NH_4^+ uptake by epilithon), whereas reduced predicted/observed $\delta^{15}N$ further from the dripper resulted from an excessive rate of NH_4^+ removal by the stream bottom. Once uptake of NH_4^+ and NO_3^- by epilithon and by the stream bottom as a whole were adjusted, predicted patterns of *Baetis* $\delta^{15}N$ reasonably approximated observed (Fig. 4D).

Predicted/observed $\delta^{15}N$ of *Prosimulium* also improved, although the underestimates early in the addition remained (Fig. 5D). The improve-

TABLE 6. Percent of N uptake as NH_4^+ by primary producers as estimated from field isotope data. Estimated $\delta^{15}N$ at the drip site for each primary producer was derived from the observed late-season transect of $\delta^{15}N$ for each taxon using the intercept of natural-log-transformed ^{15}N data. We assumed that maximum enrichment of the biota had been reached late in the addition period. $\delta^{15}NH_4^+$ was estimated from mean discharge within 1 turnover time, NH_4^+ concentration, and the known addition rate of ^{15}N.

N compartment	N turnover time (d)	$\delta^{15}NH_4^+$ at drip site (‰)	Biota $\delta^{15}N$ at drip site (‰)	% NH_4^+ uptake
Filamentous algae	8	1090	845	80
Diatoms/*Orthocladius*	5	975	460	45
Moss	all summer	1150	220	20

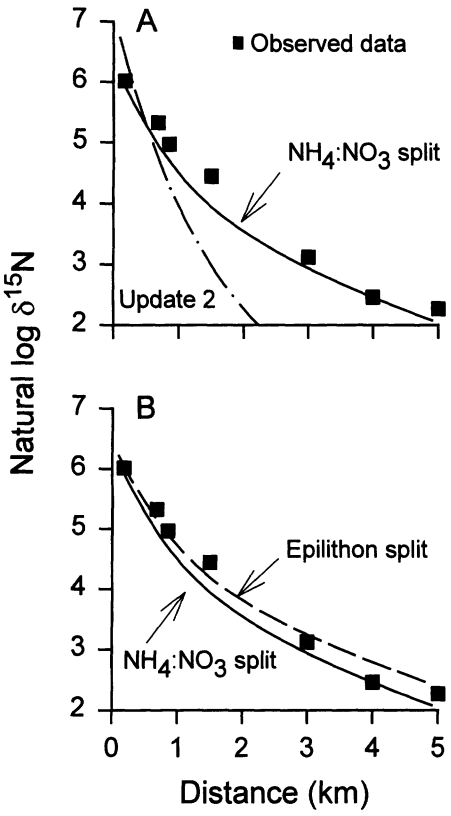

FIG. 10. Comparison of observed and model-predicted decline in natural-log-transformed $\delta^{15}N$ of *Orthocladius* on day 35 of the addition. Each calibration is based on Update 2 with changes added sequentially. Comparisons are between (A) Update 2 and a calibration that adds both NO_3^- and NH_4^+ uptake by primary producers (NH_4:NO_3 split), and (B) NH_4:NO_3 split and a calibration that separates epilithon into a diatom and epilithic detritus compartment (Epilithon split).

ment occurred because enrichment in the source compartment was reduced by ~50% when NH_4^+ preference by epilithon was reduced. This effect roughly countered the higher enrichment caused by the increased sloughing rate introduced in Update 2.

Epilithon.—The predicted epilithon compartment remained more highly labeled than the observed, even after the NH_4:NO_3 split (Fig. 11A). The field isotope data also indicated that *Baetis* was more highly labeled than the bulk epilithon on which it presumably fed (Fig. 11B). The reasonable $\delta^{15}N$ values of *Baetis* in the previous cal-

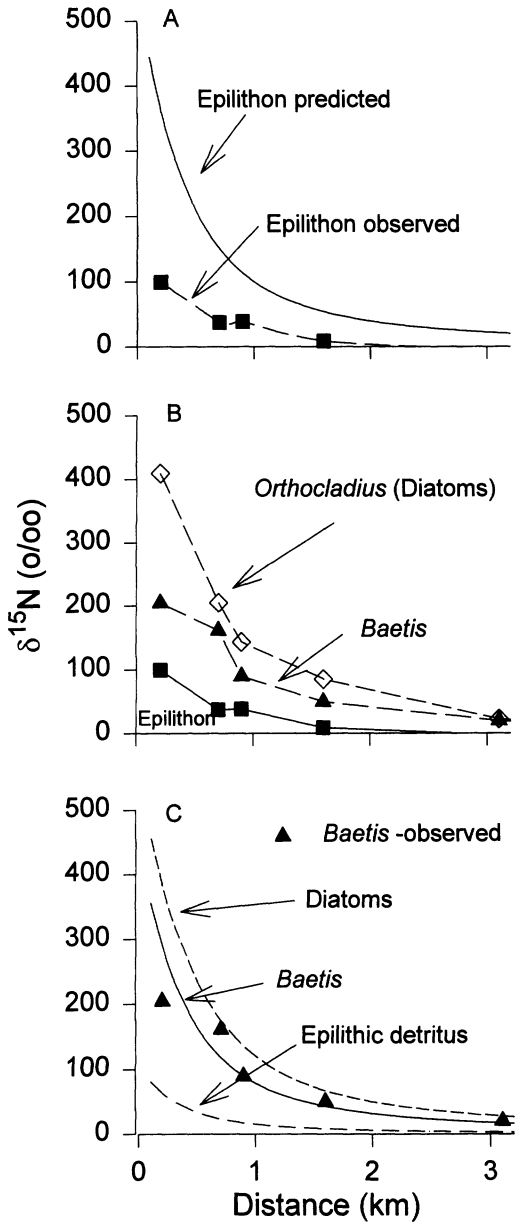

FIG. 11. Illustration of the need to split a single epilithon compartment into a fast-turnover diatom compartment and a slow-turnover epilithic detritus compartment. A.—Observed and predicted $\delta^{15}N$ of epilithon on day 35 prior to the model split of epilithon into 2 compartments. B.—Observed $\delta^{15}N$ values of *Orthocladius* (used as a surrogate for diatoms), *Baetis*, and epilithon on day 35 of the ^{15}N addition. C.—Predicted $\delta^{15}N$ values for epilithic detritus, diatoms, and *Baetis* after the division of epilithon into the fast-turnover diatom and slow-turnover epilithic detritus compartments.

ibration (Fig. 4D) were therefore achieved despite the incorrect labeling of epilithon.

Epilithon contains a mixture of algae, heterotrophic bacteria, and detrital N, which our collection method combined into 1 heterogeneous sample. In our model calibrations, the epilithon compartment became over-labeled because the ^{15}N content attributed primarily to diatom uptake could not reach equilibrium until the entire mass (including heterotrophs and detritus) was equally labeled. Clearly the diatom component would reach equilibrium quicker than the detrital component. To account for this, we divided the model epilithon into 2 compartments, a fast-turnover autotrophic compartment (diatoms) and a slow-turnover heterotrophic/detritus compartment (Table 4). Most N uptake by bulk epilithon was attributed to primary production and thus remained within the diatom compartment. We then modeled combinations of epilithic detritus and diatom uptake by *Baetis* until we achieved a reasonable correspondence between predicted and observed *Baetis* $\delta^{15}N$. A reasonable fit was achieved with a 37% epilithic detritus to 63% diatom split in diet for *Baetis* (Fig. 11D). This mix resulted in the predicted/observed $\delta^{15}N$ of *Baetis* remaining relatively unchanged compared to the previous calibration (NH_4:NO_3 split).

The division of epilithon into 2 compartments had little effect on NH_4^+-S_w because uptake rates were unchanged (Fig. 10B, Table 5). The split had little effect on the predicted $\delta^{15}N$ in *Orthocladius*, despite shifting its food source from total epilithon to diatoms alone. Both the diatom compartment in this calibration and the bulk epilithon compartment of previous calibrations attained similar levels of enrichment. Because sloughing was primarily as diatoms after splitting the compartment, predicted $\delta^{15}N$ of *Prosimulium* was also unaffected.

Dividing the epilithon compartment introduces poorly quantified stocks and fluxes, but it is consistent with the common modeling practice of partitioning bulk compartments into labile and refractory pools (Parton et al. 1983). This type of change in model structure may also prove necessary for other detrital compartments, because microbial biomass may be more enriched than bulk detritus.

Overall, NH_4^+ dynamics were tracked fairly well with the changes made in Update 3. Observed S_w over time as measured in *Orthocladius* corresponded reasonably well with predicted S_w (Fig. 12). The offset between predicted and observed S_w was not large (Fig. 12) considering we did not use the observed isotope data to derive exact NH_4^+ uptake rates.

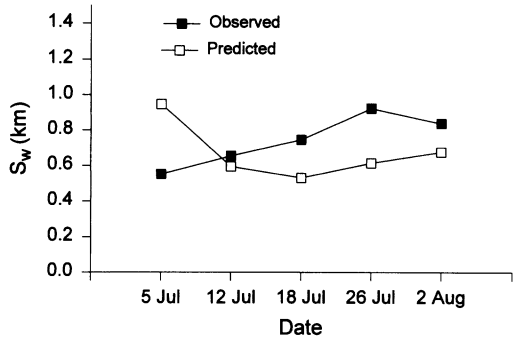

FIG. 12. Comparison of observed and predicted uptake length (S_w) over time using *Orthocladius*. Observed S_ws are based on $n = 3$ for 5 July through 26 July 1991, and $n = 4$ for 2 August 1991. Predicted estimates are from Update 3, after the isotope data have been used to assign N preference to each primary producer.

Discussion

SISTM strengths and limitations

The coupled field and modeling analysis provided a useful synoptic view of nutrient cycling along the Kuparuk River. We began by testing an N-cycle model developed without tracer information, but ultimately used the isotope data to derive certain difficult-to-measure N-cycle characteristics. Thus this study is not a rigorous validation of a pre-existing model. However, we feel the approach is simple, useful, and easily accessible even to biologists without a strong mathematical background. Our final model calibration has been applied as the a priori model for other Arctic streams to test the general applicability of the Kuparuk calibration to these other sites.

Patterns of observed isotope distribution are the result of complex interactions within the food web not easily described or understood from isotopic field data alone. SISTM can vary selected fluxes to determine their influence on isotope distribution. For example, the curvature in the plot of natural log $\delta^{15}N$ of stationary biota versus distance late in the addition (Fig. 11) re-

sulted from a combination of $^{15}N\text{-}NH_4^+$ regeneration and $^{15}N\text{-}NO_3^-$ uptake following $^{15}N\text{-}NH_4^+$ nitrification. Model experiments indicate that if nitrification rates increase, and biotic demand for NO_3^- and NH_4^+ is equal, curvature in the downstream decline of ^{15}N-biota relative to $^{15}N\text{-}NH_4^+$ increases. Model experiments have also revealed how sloughing and subsequent downstream regeneration might affect observed $^{15}N\text{-}NH_4^+$ distribution. These complex interactions are difficult to tease apart without a model to account for the numerous fluxes affecting $\delta^{15}N$ in a given compartment.

In addition to explaining complex isotopic distributions, SISTM is also useful for planning tracer experiments. Prior calibration of SISTM helped summarize current understanding of the N cycle and identify areas requiring more data. It also helped estimate the tracer requirement to label all stream compartments. Because of relatively high variability of $\delta^{15}N$ in stream N compartments during enrichment studies (B. J. Peterson, unpublished data), accurate estimation of tracer content requires an increase of roughly 10 ‰ or more in each sample type. Without the model, it is difficult to judge how much enriched NH_4^+ is required to sufficiently elevate the ^{15}N content of the large detrital N reservoirs that accumulate tracer slowly via many different pathways. Even with the model, determining this estimate can be challenging.

We stress that SISTM is a tool for analyzing the N cycle of a river and not a definitive N-cycle model of the Kuparuk River. Our ability to thoroughly test large portions of the N cycle remained limited because of the lack of isotopic field data for many compartments, especially NH_4^+, NO_3^-, DON, PON, and benthic detritus. We indirectly assessed NH_4^+ dynamics using primary producers and their grazers as indicators, but N fluxes involving NO_3^- and the detrital portion of the N cycle remained untested. In subsequent tracer additions, isotope samples of PON and benthic detritus have been collected, and $^{15}NH_4^+$ and $^{15}NO_3^-$ measurements have become available through development of new techniques (Sigman et al. 1997, Holmes et al. 1998). As a result, our ability to test and constrain fluxes in these portions of the N cycle has increased considerably since our 1991 experiment. Among the fluxes that can be estimated with the new techniques are rates of in-situ nitrification and DIN regeneration at ecosystem scales. These tracer experiments will be able to close the ^{15}N tracer budget in some cases. However, work on denitrification is still needed.

In the modeling component, we simplified the N cycle by including static fluxes. All fluxes, presented as zero-order over several weeks, must be viewed as approximate because fluxes such as NH_4^+ uptake by algae, often exhibit 1st-order or higher kinetics (Dugdale and Goering 1967, McCarthy et al. 1977, Newbold et al. 1983b, Kim et al. 1990). Use of a zero-order flux may partially explain the consistent underestimates of our model early in the addition for both *Baetis* and *Prosimulium* (Figs 4, 5). The zero-order flux model reflects our current knowledge, which lacks data on N controls and feedbacks required for a more dynamic simulation. Another simplification is the lack of hyporheic processing, which can be added as information becomes available. Despite its simplifications, our final calibration achieved a satisfactory correspondence between model predictions and the isotopic field data (Fig. 12).

Kuparuk River N cycle and future work

Despite our limited field isotope data, our field and modeling approach permits a few tentative statements about the Kuparuk N cycle. We were able to demonstrate that our early assumption, NH_4^+ preference by all primary producers, was incorrect. This result was not entirely unexpected as other stream studies have demonstrated significant NO_3^- uptake (Munn and Meyer 1990, Marti et al. 1997). Our assumption was a preliminary simplification given the lack of information in Alaskan streams, and the fact that N did not appear to be limiting (Peterson et al. 1983). After deriving the NH_4:NO_3 preference for each primary producer, we achieved good correspondence between observed and predicted S_w, indicating that our estimate of total N uptake based on measurements during the field study was reasonable.

A 2nd insight derived from modeling was that primary production probably dominates N uptake in the Kuparuk River. In our final model calibration, 65% of midsummer NH_4^+ uptake was attributed to primary producers (Appendix), with the remainder attributed to other processes, such as nitrification. High N uptake by primary producers is expected because these streams are unshaded and experience continu-

ous light during the summer growing season. This result contrasts with P dynamics of shaded streams like Walker Branch, where most nutrient uptake is heterotrophic (Newbold et al. 1983a, Mulholland et al. 1985).

SISTM is a tool to develop understanding of N cycles in specific stream ecosystems. It is not a simulation model that might, for example, predict N-cycle characteristics under different N loading or climatic conditions. Future development is required of mechanistic models designed to predict the biogeochemical and food-web consequences of climate change or shifts in N, P, and organic matter loading. The coupled modeling and field approach discussed here can be applied equally well with a more dynamic, process model.

Process models must incorporate controls and feedbacks that can only be elucidated by laboratory and field perturbation experiments such as whole-stream nutrient additions (e.g., Elwood et al. 1981, Newbold et al. 1983b, Peterson et al. 1993), nutrient-uptake kinetic studies (e.g., Kim et al. 1990, 1992), and intensive microbial and food-web experimentation (e.g., Mulholland et al. 1994). Whole-ecosystem tracer studies and the compartment model presented here lack this information. They do describe current N-cycle characteristics and, via modeling, fill in the many gaps between field measurements and what composes the entire cycle in nature. These steps are important in developing the understanding needed to create and test realistic simulation models. Currently a 10-stream intersite comparison (LINX) using the coupled field and modeling analysis of N cycling is underway. These ^{15}N field datasets are accompanied by intensive hydrologic and biotic sampling data and will be valuable to develop and then test general simulation models of stream N dynamics. A valid simulation model should be able to predict the distribution of ^{15}N following a tracer addition even more accurately than the static box model, which uses less information and lacks controls and feedbacks. We believe that the development of watershed-scale biogeochemical and food-web simulation models should be a long-term goal for future research. Simulation models with documented predictive capability are needed to produce information about the future status of streams and rivers under the variety of local and global changes that impact these ecosystems now and in coming decades.

Acknowledgements

This research was funded by NSF grants OPP-9024188, OPP-9400722, BSR-870232, and DEB 9211775 and is a contribution to the NSF Arctic LTER Program. We thank the staff of the Toolik Lake Field Station for logistical support, Carolyn Bauman and Heidi Golden for field work, and Kris Tholke for the ^{15}N analyses. We also thank the reviewers of this paper for their helpful suggestions.

Literature Cited

AMINOT, A., D. S. KIRKWOOD, AND R. KEROUEL. 1997. Determination of ammonia in seawater by the indophenol-blue method: evaluation of the ICES NUTS I/C 5 questionnaire. Marine Chemistry 56: 59–75.

ARSCOTT, D. B. 1997. Primary production in a 4th order arctic stream. MS Thesis, University of New Hampshire, Durham, New Hampshire.

BALL, R. C., AND F. F. HOOPER. 1963. Translocation of phosphorous in a trout stream ecosystem. Pages 217–228 *in* V. Schultz and A. W. Klement (editors). Radioecology. Reinhold, New York.

BOWDEN, W. B., B. J. PETERSON, J. C. FINLAY, AND J. TUCKER. 1992. Epilithic chlorophyll a, photosynthesis, and respiration in control and fertilized reaches of a tundra stream. Hydrobiologia 240: 121–131.

CUSHING, C. E., G. W. MINSHALL, AND J. D. NEWBOLD. 1993. Transport dynamics of fine particulate organic matter in two Idaho streams. Limnology and Oceanography 38:1101–1115.

DUGDALE, R. C., AND J. J. GOERING. 1967. Uptake of new and regenerated forms of nitrogen in primary productivity. Limnology and Oceanography 12:192–206.

ELWOOD, J. W., J. D. NEWBOLD, A. F. TRIMBLE, AND R. W. STARK. 1981. The limiting role of phosphorous in a woodland stream ecosystem: effects of P enrichment on leaf decomposition and primary producers. Ecology 62:146–158.

EPPLEY, R. W. 1972. Temperature and phytoplankton growth in the sea. U.S. National Marine Fisheries Service Fishery Bulletin 70:1063–1085.

GALLOWAY, J. N., W. H. SCHLESINGER, H. LEVY, A. MICHAELS, AND J. L. SCHNORR. 1995. Nitrogen fixation: atmospheric enhancement—environmental response. Global Biogeochemical Cycles 9:235–252.

GOLTERMAN, H. L., AND R. S. CLYMO. 1969. Methods for the chemical analysis of freshwaters. International Biological Program. Volume No. 8. Blackwell Scientific Publications Ltd., Oxford, UK.

HALL, R. O., B. J. PETERSON, AND J. L. MEYER. 1998.

Testing a nitrogen-cycling model of a forest ecosystem using a nitrogen-15 tracer addition. Ecosystems 1:283–298.

HERSHEY, A. E., AND A. L. HILTNER. 1988. Effect of a caddisfly on black fly density: interspecific interactions limit black flies in an arctic river. Journal of the North American Benthological Society 7: 188–196.

HERSHEY, A. E., A. L. HILTNER, M. A. J. HULLAR, M. C. MILLER, J. R. VESTAL, M. A. LOCK, S. RUNDLE, AND B. J. PETERSON. 1988. Nutrient influence on a stream grazer: *Orthocladius* microcommunities respond to nutrient input. Ecology 69:1383–1392.

HERSHEY, A. E., J. PASTOR, B. J. PETERSON, AND G. W. KLING. 1993. Stable isotopes resolve the drift paradox for *Baetis* mayflies in an Arctic river. Ecology 74:2315–2325.

HOLMES, R. M., J. W. MCCLELLAND, D. M. SIGMAN, B. FRY, AND B. J. PETERSON. 1998. Measuring ^{15}N-NH_4^+ in marine, estuarine, and fresh waters: an adaptation of the ammonia diffusion method for samples with low ammonium concentrations. Marine Chemistry 60:235–243.

HOLMES, R. M., B. J. PETERSON, L. A. DEEGAN, J. E. HUGHES, AND B. FRY. Nitrogen cycling in the oligohaline zone of New England estuary. Ecology (in press).

HOWARTH, R. W., G. BILLEB, D. SWANEY, A. TOWNSEND, N. JARWORSKI, K. LATHJA, J. A. DOWNING, R. ELMGREN, N. CARACO, T. JORDAN, F. BERENDSE, J. FRENEY, V. KUDEYAROV, P. MURDOCH, AND Z. ZHAO-LIANG. 1996. Regional nitrogen budgets and riverine inputs of N and P for the drainages to the North Atlantic Ocean: natural and human influences. Biogeochemistry 35:75–139.

JORDAN T. E., AND D. E. WALLER. 1996. Human contributions to terrestrial N-flux. BioScience 46: 655–664.

KIM, B. K. A., A. P. JACKMAN, AND F. J. TRISKA. 1990. Modeling transient storage and nitrate uptake kinetics in a flume containing a natural periphyton community. Water Resources Research 26:505–515.

KIM, B. K. A., A. P. JACKMAN, AND F. J. TRISKA. 1992. Modeling biotic uptake by periphyton and transient hyporheic storage of nitrate in a natural stream. Water Resources Research 28:2743–2752.

KLING, G. W. 1994. Ecosystem-scale experiments in freshwaters: the use of stable isotopes. Pages 91–120 *in* L. A. Baker (editor). Environmental chemistry of lakes and reservoirs. Advances in Chemistry Series. Volume 237. American Chemical Society, Washington, DC.

KNADELHOFFER, K. J., M. R. DOWNS, B. FRY, J. D. ABER, A. H. MAGILL, AND J. M. MELILLO. 1995. The fate of ^{15}N labeled nitrate additions to a northern hardwood forest in eastern Maine, USA. Oecologia 103:292–301.

MARTI, E., N. B. GRIMM, AND S. G. FISHER. 1997. Pre- and post-flood retention efficiency of nitrogen in a Sonoran Desert stream. Journal of the North American Benthological Society 16:805–819.

MARTI, E., AND F. SABATER. 1996. High variability in temporal and spatial nutrient retention in Mediterranean streams. Ecology 77:854–869.

MCCARTHY, J. J., W. R. TAYLOR, AND J. L. TAFT. 1977. Nitrogenous nutrition of the plankton in Chesapeake Bay. 1. Nutrient availability and phytoplankton preferences. Limnology and Oceanography 22:996–1011.

MEYBECK, M. 1982. Carbon, nitrogen, and phosphorous transport by world rivers. American Journal of Science 282:401–450.

MEYER, J. L., AND G. E. LIKENS. 1979. Transport and transformation of phosphorous in a forest stream ecosystem. Ecology 60:1255–1269.

MULHOLLAND, P. J., J. D. NEWBOLD, J. W. ELWOOD, AND L. A. FERREN. 1985. Phosphorous spiralling in a woodland stream: seasonal variations. Ecology 66:1012–1023.

MULHOLLAND, P. J., A. D. STEINMAN, E. R. MARZOFF, D. R. HART, AND D. L. DEANGELIS. 1994. Effect of periphyton biomass on hydraulic characteristics and nutrient cycling in streams. Oecologia 98:40–47.

MUNN, N. L., AND J. L. MEYER. 1990. Habitat-specific solute retention in two small streams: an intersite comparison. Ecology 71:2069–2082.

NEWBOLD, J. D., J. W. ELWOOD, R. V. O'NEILL, AND A. L. SHELDON. 1983a. Phosphorous dynamics in a woodland stream ecosystem: a study of nutrient spiralling. Ecology 64:1249–1265.

NEWBOLD, J. D., J. W. ELWOOD, R. V. O'NEILL, AND W. VAN WINKLE. 1981. Measuring nutrient spiralling in streams. Canadian Journal of Fisheries and Aquatic Sciences 38:860–863.

NEWBOLD, J. D., J. W. ELWOOD, M. S. SCHULZE, R. W. STARK, AND J. C. BARMEIER. 1983b. Continuous ammonium enrichment of a woodland stream: uptake kinetics, leaf decomposition, and nitrification. Freshwater Biology 13:193–204.

PARTON, W. J., D. W. ANDERSON, C. V. COLE, AND J. W. B. STEWART. 1983. Simulation of soil organic matter formation and mineralization in semiarid agroecosystems. Pages 533–550 *in* R. R. Lowrance, R. L. Todd, L. E. Asmussen, and R. A. Leonard (editors). Nutrient cycling in agricultural ecosystems. Special Publication No. 23. University of Georgia, College of Agriculture, Agricultural Experiment Stations, Athens, Georgia.

PETERSON, B. J., J. DEEGAN, J. HELFRICH, J. HOBBIE, M. HULLAR, B. MOLLER, T. FORD, A. HERSHEY, A. HILTNER, G. KIPPHUT, M. A. LOCK, D. M. FIEBIG, V. MCKINLEY, M. C. MILLER, J. R. VESTAL, R. VENTULLO, AND G. VOLK. 1993. Biological responses

of a tundra river to fertilization. Ecology 74:653–672.

PETERSON, B. J., J. E. HOBBIE, AND T. L. CORLISS. 1986. Carbon flow in a tundra stream ecosystem. Canadian Journal of Fisheries and Aquatic Sciences 43:1259–1270.

PETERSON, B. J., J. E. HOBBIE, T. L. CORLISS, AND K. KRIET. 1983. A continuous-flow periphyton bioassay: tests of nutrient limitation in a tundra stream. Limnology and Oceanography 28:583–591.

PETERSON, B. J., G. W. KLING, AND M. BAHR. 1997. A tracer investigation of nitrogen cycling in a pristine tundra river. Canadian Journal of Fisheries and Aquatic Sciences 54:2361–2367.

REDFIELD, A. C. 1958. The biological control of chemical factors in the environment. American Scientist 46:205–221.

SIGMAN, D. M., M. A. ALTABET, R. MICHENER, D. C. MCCORKLE, B. FRY, AND R. M. HOLMES. 1997. Natural abundance-level measurement of the nitrogen isotopic composition of oceanic nitrate: an adaptation of the ammonia diffusion method. Marine Chemistry 57:227–242.

SMOCK, L. A. 1980. Relationships between body size and biomass of aquatic insects. Freshwater Biology 110:3375–3383.

STERNER, R. W., AND D. O. HESSEN. 1994. Algal nutrient limitation and the nutrition of aquatic herbivores. Annual Review of Ecology and Systematics 25:1–29.

STREAM SOLUTE WORKSHOP. 1990. Concepts and methods for assessing solute dynamics in stream ecosystems. Journal of the North American Benthological Society 9:95–119.

TRISKA, F. J., V. C. KENNEDY, R. J. AVANZINO, G. W. ZELLWEGER, AND K. E. BENCALA. 1989a. Retention and transport of nutrients in a third order stream: channel processes. Ecology 70:1877–1892.

TRISKA, F. J., V. C. KENNEDY, R. J. AVANZINO, G. W. ZELLWEGER, AND K. E. BENCALA. 1989b. Retention and transport of nutrients in a third order stream in northwestern California: hyporheic processes. Ecology 70:1893–1905.

VALETT, H. M., J. A. MORRICE, C. N. DAHM, AND M. E. CAMPANA. 1996. Parent lithology, surface-groundwater exchange, and nitrate retention in headwater streams. Limnology and Oceanography 41:333–345.

VITOUSEK, P. M. 1994. Beyond global warming: ecology and global change. Ecology 75:1861–1876.

VITOUSEK, P. M., J. D. ABER, R. W. HOWARTH, G. E. LIKENS, P. A. MATSON, D. W. SCHINDLER, W. H. SCHLESINGER, AND D. G. TILMAN. 1997. Human alteration of the global nitrogen cycle: sources and consequences. Ecological Applications 7:737–750.

WEBSTER, J. R., D. J. D'ANGELO, AND G. T. PETERS. 1991. Nitrate and phosphate uptake in streams at Coweeta Hydrologic Laboratory. Verhandlungen der Internationalen Vereinigung für theoretische und angewandte Limnologie 24:1681–1686.

Received: 16 April 1998
Accepted: 6 April 1999

APPENDIX. The matrix of fluxes (mg N m^{-2} d^{-1}) used in Update 3 (after including isotope data to determine N preference and to divide bulk epilithon into diatom and epilithic detritus compartments) for the reference reach of the Kuparuk River during the 1991 ^{15}N tracer addition. NO_3^- = nitrate, NH_4^+ = ammonium, DON = dissolved organic nitrogen, PON = particulate organic nitrogen, DTR = benthic detritus, MOS = moss, ALG = filamentous algae, DIA = diatoms, EPI = epilithic detritus, BRA = *Brachycentrus*, BLK = *Prosimulium*, BAE = *Baetis* sp., RHY = *Rhyacophila* sp., YOY = young-of-the-year grayling, GRA = adult grayling, ORT = *Orthocladius*, CHI = other chironomids. Upstream inputs are variable with a median for NH_4^+ of 181,000 mg N/d and for NO_3^- 725,000 mg N/d. Lateral inputs of NH_4^+ = 12.94 mg N m^{-2} d^{-1} and of NO_3^- = 4.11 mg N m^{-2} d^{-1}. To convert lateral inputs to mg N m^{-1} d^{-1} multiply by stream width (17 m). Flux units between water column compartments (NO_3^-, NH_4^+, DON, PON) are given in units per m^2. To convert these fluxes to per unit volume, divide by depth (0.4 m).

	Sink							
	NO_3^-	NH_4^+	DON	PON	DTR	MOS	ALG	DIA
Source								
NO_3^-	0	0	0	0	0	1.06	0.71	17.06
NH_4^+	7.65	0	0	0	1.18	0.29	2.82	14.12
DON	0	0	0	0	2.68	0	0	0
PON	0	0.02	0.02	0	106.19	0	0	0
DTR	7.06	10.59	2.94	79.62	0	0	0	0
MOS	0	0	0.14	0	1.22	0	0	0
ALG	0	0	0.35	0	3.18	0	0	0
DIA	0	0	3.12	25.24	0	0	0	0
EPI	0	0	0.18	3.24	0	0	0	0
BRA	0	0.03	0	0.03	0	0	0	0
BLK	0	1.47	0	1.47	1.18	0	0	0
BAE	0	0.12	0	0.12	0	0	0	0
RHY	0	0.01	0	0.01	0.01	0	0	0
YOY	0	0.35	0	0.29	0.35	0	0	0
GRA	0	0.06	0	0.06	0.06	0	0	0
ORT	0	0.24	0	0.24	0.24	0	0	0
CHI	0	0.35	0	0.32	0	0	0	0
Sum	14.71	13.24	6.75	110.64	116.29	1.35	3.53	31.18

APPENDIX. Extended.

Sink									
EPI	BRA	BLK	BAE	RHY	YOY	GRA	ORT	CHI	Sum
0	0	0	0	0	0	0	0	0	18.83
0.12	0	0	0	0	0	0	0	0	26.18
2.76	0	0	0	0	0	0	0	0	5.44
0	0.12	4.12	0	0	0	0	0	0	110.47
0	0	0	0	0	0	0	0	0.47	100.68
0	0	0	0	0	0	0	0	0	1.36
0	0	0	0	0	0	0	0	0	3.53
1.18	0	0	0.47	0	0	0	0.71	0.47	31.19
0	0	0	0.24	0	0	0	0	0.41	4.07
0	0	0	0	0	0	0.06	0	0	0.12
0	0	0	0	0	0	0	0	0	4.12
0	0	0	0	0	0.41	0.06	0	0	0.71
0	0	0	0	0	0	0	0	0	0.03
0	0	0	0	0	0	0	0	0	0.99
0	0	0	0	0	0	0	0	0	0.18
0	0	0	0	0	0	0	0	0	0.72
0	0	0	0	0.03	0.59	0.06	0	0	1.35
4.06	0.12	4.12	0.71	0.03	1.00	0.18	0.71	1.35	